# The deep atmosphere of Venus and the possible role of density-driven separation of $CO_2$ and $N_2$

Sebastien Lebonnois,<sup>1\*</sup> Gerald Schubert<sup>2</sup>

<sup>1</sup>Laboratoire de Météorologie Dynamique (LMD/IPSL), Sorbonne Universités, UPMC Univ Paris 06, ENS, PSL Research University, Ecole Polytechnique, Université Paris Saclay, CNRS, Paris, France <sup>2</sup>Department of Earth, Planet. and Space Sci., UCLA, CA, USA

\*e-mail: sebastien.lebonnois@lmd.jussieu.fr.

With temperatures around 700 K and pressures of around 75 bar, the deepest 12 kilometres of the atmosphere of Venus are so hot and dense that the atmosphere behaves like a supercritical fluid. The Soviet VeGa-2 probe descended through the atmosphere in 1985 and obtained the only reliable temperature profile for the deep Venusian atmosphere thus far. In this temperature profile, the atmosphere appears to be highly unstable at altitudes below 7 km, contrary to expectations. We argue that the VeGa-2 temperature profile could be explained by a change in the atmospheric gas composition, and thus molecular mass, with depth. We propose that the deep atmosphere consists of a non-homogeneous layer in which the abundance of  $N_2$  - the second most abundant constituent of the Venusian atmosphere after  $CO_2$  - gradually decreases to near-zero at the surface. It is difficult to explain a decline in  $N_2$  towards the surface with known nitrogen sources and sinks for Venus. Instead we suggest,

10

11

12

13

partly based on experiments on supercritical fluids, that density-driven separation of  $N_2$  from  $CO_2$  can occur under the high pressures of Venus's deep atmosphere, possibly by molecular diffusion, or by natural density-driven convection. If so, the amount of nitrogen in the atmosphere of Venus is 15% lower than commonly assumed. We suggest that similar density-driven separation could occur in other massive planetary atmospheres.

Venus has a massive and scorching atmosphere. With a surface pressure of 92 bars its atmosphere is 92 times as massive as Earth's atmosphere. At the surface of Venus the temperature is 464°C, hot enough to melt lead. Atmospheric density at the surface is about 65 kg m<sup>-3</sup> or 6.5% the density of liquid water.<sup>1</sup> Atmospheric composition is 96.5% CO<sub>2</sub> and 3.5% N<sub>2</sub> (by volume).<sup>2</sup> Minor gases include SO<sub>2</sub>, Ar, H<sub>2</sub>O, and CO.<sup>3,4</sup> SO<sub>2</sub> at the level of only 150 ppm is particularly important because of the blanket of sulfuric acid clouds that completely shroud the planet from view.<sup>5</sup> The clouds effectively reflect the solar radiation incident on Venus resulting in a bond albedo of 0.77, more than double that of the Earth at 0.31. As a consequence more sunlight is absorbed at the surface of Earth than at Venus' surface even though Venus is 72% nearer to the Sun. The temperature distribution in Venus' atmosphere is determined in large part by its absorption of sunlight.<sup>1</sup> Temperature and pressure are so large at Venus' surface that the atmosphere is a supercritical fluid.

In addition to the basic properties above we have detailed knowledge of the atmospheric structure (altitude profiles of temperature and pressure and locations of the clouds) from decades of observation by orbiting spacecraft (Soviet Venera 15 and 16,<sup>6–8</sup> U.S. Pioneer Venus Orbiter<sup>9,10</sup> and Magellan,<sup>11</sup> ESA Venus-Express<sup>12–14</sup> and the ongoing Japanese Akatsuki), entry probes and landers,<sup>15–18</sup> balloons,<sup>17</sup> and Earth-based telescopes<sup>3,19–21</sup> (Fig. 1). These observations have shown that Venus, like Earth, has a troposphere extending from the surface to the upper cloud region at about 60 to 65 km altitude, wherein temperature decreases with height.<sup>1,22</sup>

The sulfuric acid clouds extend downward to about 48 km altitude.<sup>5</sup> Above the clouds are regions of the atmosphere analogous to Earth's mesosphere and thermosphere but our focus here is the atmosphere below the clouds. At cloud heights atmospheric temperature and pressure are similar to those at the Earth's surface. There is no stratosphere on Venus similar to Earth's stratosphere that is heated by ozone absorption of solar ultraviolet radiation.

The altitude profile of temperature allows identification of stable layers and layers of convective activity. There is a convective region in the clouds between about 50 and 55 km altitude, <sup>14,23</sup> as experienced by the Soviet VeGa-1 and VeGa-2 balloons that cruised in this layer. <sup>17</sup> Below this region extending downward to about 32 km altitude the atmosphere is stable. Below this stable layer the atmosphere is well mixed down to an altitude of about 18 km. At even greater depth, the atmosphere is stable again until an altitude of about 7 km. The nature of the lowest 7 km of the atmosphere, a layer that contains 37% of the mass of the atmosphere, is at the heart of our discussion.

While the exploration of Venus' atmosphere has been extensive, as discussed above, the deep atmosphere remains a largely unobserved region. It is challenging to obtain data remotely below the thick cloud layer covering the planet. Many probes have been sent to the surface of Venus: the Soviet Venera mission series, 15 the U.S. Pioneer Venus probes, 16 and the Soviet VeGa probes. 17, 18 These probes measured temperature (T) and pressure (p) during descent, and made measurements of atmospheric composition, showing that the two major constituents were carbon dioxide  $(CO_2, 96.5\%)$  and nitrogen  $(N_2, 3.5\%)$ . 2,24,25 Unfortunately, almost no temperature data were obtained from the deepest layers of Venus' atmosphere, since most Venera probe temperature profiles had large uncertainties and all the Pioneer Venus probe temperature experiments stopped functioning at 12 km above the surface. The Pioneer Venus temperature profiles below 12 km were reconstructed from pressure measurements, extrapolation of T(p) and iterative altitude computation, 16 and only these reconstructions (prone to significant

uncertainties) and the Venera 10 profile<sup>26</sup> were used to build the Venus International Reference
Atmosphere model.<sup>22</sup> The only available and reliable temperature profile reaching to the surface
was acquired by the VeGa-2 probe<sup>17,18,27</sup> (Fig. 2). Measurements were done with two different
platinum wires (one bare, one protected in a thin ceramic shield), with a measured accuracy
of ±0.5 K from 200 to 800 K. The time constants of the two detectors were 0.1 s and 3 s.
The delay of the second detector induced systematic shift between the two measurements, with
differences no larger than 2 K down to the surface.<sup>17</sup> The measured temperature profile fits remarkably well with the Pioneer Venus and VIRA profiles above roughly 15 km altitude.<sup>27</sup> This
illustrates the small temporal and spatial variability of the temperature in the deep atmosphere
of Venus, with differences between the different observed profiles smaller than 5 K (and not
depending on altitude).

Below 7 km, a region where no precise measurements of  $N_2$  abundance was published,<sup>2</sup> the VeGa-2 temperature profile showed a strongly unstable vertical temperature gradient that has remained unexplained since VeGa-2 landed on Venus on June 15, 1985.<sup>27,28</sup> The difference in temperature between the adiabatic profile (neutral stability) and the observed profile is up to roughly 9 K around 7 km. This interface region between the surface and the atmosphere, called the planetary boundary layer (PBL), controls how the angular momentum and energy are exchanged between the two reservoirs. Characterization of the mixing processes occuring in the PBL is crucial to understanding the angular momentum budgets of the atmosphere and solid planet. This is particularly true in the case of Venus, which is characterized by a peculiar atmospheric circulation, the superrotation: the whole atmosphere is rotating much faster than the surface below, with maximum zonal winds reaching more than 100 m/s at the altitude of the cloud top (70 km).<sup>29</sup> This large zonal rotation of the massive Venus atmosphere makes its atmospheric angular momentum a relatively large fraction  $(1.6 \times 10^{-3})$  of the angular momentum of the solid body. For Earth this fraction is  $2.7 \times 10^{-8}$ . Exchanges of angular momentum between

the two reservoirs would lead to changes in the length of day of Venus and zonal wind speeds in the atmosphere.

A possible interpretation of this peculiar temperature structure involves unexpected properties of the CO<sub>2</sub>/N<sub>2</sub> mixture in high-pressure, high-temperature conditions, which are not well known. This is illustrated by a recent experiment that shows a vertical separation between these two compounds within the fluid phase, a behavior difficult to explain.<sup>30</sup> Despite a lack of theoretical and experimental constraints, this density-driven separation may be the key to understanding the structure of the deepest layers of Venus' atmosphere.

#### 97 Stability in the deep atmosphere of Venus

The temperature profile close to the surface is a very good indicator of the properties of the PBL. In addition to the static stability, the potential temperature is an efficient variable to analyze the stratification of the atmosphere (Box 1). The vertical profiles of the potential temperature derived from the VeGa-2 and Pioneer Venus probes are displayed in Fig. 3. Layers with constant 101 potential temperature are layers where the temperature follows the adiabatic lapse rate, indica-102 tive of convection or large-scale vertical mixing. Below roughly 7 km, the vertical gradient of 103 the VeGa-2 potential temperature is approximately constant and strongly negative (-1.5K/km), 104 corresponding to a highly unstable situation. Such a profile of potential temperature is never 105 observed on Earth. On Mars, radiative surface heating sometimes drives a very unstable surface 106 layer, yielding highly active convection up to 9 km above surface. In these conditions, the po-107 tential temperature may display negative gradients over the surface, up to 1 or 2 km altitude.<sup>31</sup> 108 For Venus, this situation is unlikely, as direct heating of the surface is only a small fraction of 109 that of Mars' surface.32 110

However, the VeGa-2 probe potential temperature profile can be understood if the stability of this layer is altered by a vertical gradient in the mean molecular mass  $(\mu)$ , i.e., in the atmospheric

gas composition (as detailed in the online Methods section): the assumption that this layer is close to convective instability yields a vertical profile of mean molecular mass which is almost linear with the logarithm of pressure, from 43.44 g/mol above 7 km to 44.0 g/mol at the surface.

#### 16 A density-driven gas separation hypothesis

134

135

Though a systematic error in the temperature measurements can not be excluded, the fact that 117 this error would have maintained a stable vertical temperature gradient from 7 km altitude to 118 the surface, for both VeGa-2 temperature sensors is unlikely. If this temperature profile is 119 accurate, then it may be neutrally stable with the previously mentioned variation in the mean 120 molecular mass  $\mu$ . The value obtained in this case for  $\mu$  at the surface is remarkably close 121 to that of pure CO<sub>2</sub>, so that an intriguing, but very simple explanation for the vertical profile 122 of  $\mu$  is a regular decrease in  $N_2$  mole fraction, from 3.5% above 7 km to almost zero at the surface. Such a composition variation would have a significant impact on the total amount of nitrogen contained in the atmosphere, which would decrease to only 85% of the total amount for 125 a well mixed atmosphere. This could have potential implications for studies that investigate the 126 respective nitrogen inventories of Earth and Venus.<sup>33</sup> The increase of the mean molecular mass 127 towards the surface might also be consistent with an increase in the abundance of an atmospheric 128 compound heavier than CO<sub>2</sub>, though this would be an even more puzzling coincidence. For an 129 increase up to the 0.1% level at the surface, the molar mass of the component would need to 130 be of the order of 560 g/mol. A lower molar mass would mean a higher abundance. Solutions 131 could be found, but it seems quite unlikely that the change of composition would be different 132 from the decrease of N<sub>2</sub> abundance as the surface is approached. 133

Based on this hypothetical interpretation of the VeGa-2 probe temperature profile, the gradient in  $N_2$  abundance obtained in Venus's deep atmosphere is around 5 ppm/m. In planetary atmospheres, such vertical gradients of composition are usually associated with sources or sinks

of the varying compound, such as chemistry, condensation, or surface processes. However, the hypothesis that this nitrogen gradient might be the result of a surface sink faces serious difficulties. It would require a constant downward flux of nitrogen, that would need to be sustained over geological times unless a recycling process or an equivalent source could drive nitrogen back into the atmosphere.

Another possibility is explored here: this gradient may result from an equilibrium state due 142 to separation of nitrogen from carbon dioxide in the dense conditions of Venus's deep atmo-143 sphere. Such a separation of N<sub>2</sub> and CO<sub>2</sub> in high-pressure conditions is illustrated by recent ex-144 periments.<sup>30,34</sup> Though the conditions of these experiments are clearly different from conditions 145 in the deep atmosphere of Venus, it demonstrates the impact of high densities on the CO<sub>2</sub>/N<sub>2</sub> binary mixture. In the first of these experiments, 30 a mixture of 50% N<sub>2</sub>/50% CO<sub>2</sub> (mole fractions) was put in an 18-cm high vessel at room temperature for pressures above 100 bars. At 148 p=100 bars and T=23°C, the CO<sub>2</sub>/N<sub>2</sub> mixture is supercritical, not far above the critical point of the fluid mixture ( $T_C = -9.3^{\circ}$ C,  $p_C = 98$  bar), and CO<sub>2</sub> departs slightly from being 150 ideal. Using the equations of state for pure CO<sub>2</sub> and N<sub>2</sub>, <sup>34,35</sup> CO<sub>2</sub> partial pressure is 44 bars, 151 CO<sub>2</sub> density is 101 kg/m<sup>3</sup> and total density in the vessel is around 165 kg/m<sup>3</sup>, to be compared 152 with the densities in the deep Venusian atmosphere: 40 to 70 kg/m<sup>3</sup> for pressures higher than 153 50 bars. In these experimental conditions, N<sub>2</sub> and CO<sub>2</sub> were observed to separate significantly along the vertical dimension, N2 reaching over 70% mole fraction at the top of the vessel, while CO<sub>2</sub> reached almost 90% at the bottom.<sup>30</sup> Over the 18 cm of the experimental vessel, this sep-156 aration is extreme, with an average gradient of 3 to 4%/cm. In Venus's deep atmosphere, the 157 5 ppm/m gradient in N<sub>2</sub> abundance appears much smaller in comparison. 158

The molecular diffusion in this binary gas mixture includes three terms: one due to the compositional gradient, one due to the temperature gradient, and one due to the pressure gradient. The amplitude of this pressure term is controlled by the barodiffusion coefficient  $k_p$ .

Molecular diffusion in an ideal gas mixture increases as the pressure decreases towards higher altitudes, the expression of  $k_p$  is known for an ideal binary gas mixture, and turbulent diffusion in usual atmospheric conditions is strong enough to homogenize atmospheric composition up to 164 the homopause. At this level, molecular diffusion dominates and the barodiffusion induces mass 165 separation of the different compounds. Could high-pressure conditions and departure from the 166 ideal gas law induce strongly non-linear behavior of the barodiffusion coefficient? For such 167 a gradient to be maintained in the near-surface layer of Venus's atmosphere against large-scale 168 and turbulent mixing, the barodiffusion coefficient  $k_p$  would need to be several orders of mag-169 nitude larger than for an ideal gas in the same conditions, which may seem highly unlikely. It 170 is also the case for the previously detailed experiment.<sup>30</sup> Unfortunately, no measured or theo-171 retical values are yet available for  $k_p$ , neither for the experimental set-up<sup>30</sup> nor for Venus's deep 172 atmospheric conditions. In the experiments, <sup>30,34</sup> natural density-driven convection is mentioned 173 as a possible driver, inducing transport of nitrogen-rich lighter parcels upward while CO<sub>2</sub>-rich 174 heavier parcels would move downward. Additional experimental and theoretical studies are 175 clearly needed to investigate this possibility and to solve this puzzle. 176

#### Dynamics of the deep atmosphere of Venus

To better understand the dynamical state of the different atmospheric layers, as well as the behavior of the PBL near the surface of Venus, the atmospheric circulation was explored using the *Laboratoire de Meteorologie Dynamique* (LMD) Venus General Circulation Model (GCM).<sup>37</sup>

The variation of the mean molecular mass with pressure in the deep atmosphere was implemented in the computation of the potential temperature within the GCM, though this modification only slightly affects the dynamical state of the deepest layers. Fitting the observed
temperature structure in detail with a radiative transfer model is challenging, because of the
sensitivity of the temperature profile to many parameters that are not well known.<sup>38</sup> However,

with a fine tuning of these parameters (detailed in the online Methods section), the GCM is able to reproduce the vertical structure of the potential temperature. Therefore, the mean meridional circulation and the turbulent activity diagnosed by the GCM (Fig. 4) can be used to evaluate the dynamical conditions within the atmosphere, including the deepest layer discussed here, despite the large difficulty to get observational constraints for this region.

The deepest layer (below 8 km) is close to neutral stability. In the simulation, it is slightly 191 turbulent only near its top, and near the surface with a diurnal convective layer that reaches 1 192 to 2 km above the surface around noon local time. This result of the GCM radiative transfer 193 is obtained both when taking into account the composition variation and when composition is 194 uniform. The mean meridional circulation participates in the mixing of the energy through a 195 surface Hadley-type cell roughly 7-km thick. This is similar to the 2-km thick seasonal PBL 196 observed on Titan by the Huygens probe, associated with the mixing by the deepest mean 197 meridional circulation cells.<sup>39</sup> The hypothetical separation of N<sub>2</sub> and CO<sub>2</sub> that would explain the 198 VeGa-2 potential temperature profile in the deepest layer needs to occur on timescales shorter 199 than the dynamical overturning of this surface cell ( $\tau_{dyn} = L/\overline{v}$ , where  $L \sim 10^4$  km is the 200 horizontal size of the cell and  $\overline{v}\sim 0.05$  m/s is the mean meridional wind near the surface, 201 yielding  $\tau_{dyn} \sim 2 \times 10^8$  s, or 20 Vd) in order to maintain this vertical gradient in the atmospheric 202 composition, while the layer is close to convective instability. The simulation confirms the very 203 small spatial and temporal variations of the temperature profile, with a diurnal cycle only active near the surface.

#### Dense gas separation at Venus and beyond

The unexplained behavior of the  $CO_2/N_2$  mixture in the temperature and pressure conditions of the deep atmosphere of Venus needs to be confirmed. First, it illustrates how important it is to go back to Venus to make additional in-situ measurements down to the surface. Second, further studies are needed, both theoretical and experimental. The compositional gradient deduced from our interpretation of the VeGa-2 profile (5 ppm/m) could be measured in a large experimental tank where Venus' atmospheric conditions can be reproduced. Such a result could trigger interest for theoretical and experimental studies dedicated to other binary mixtures, that could be relevant for the high-pressure atmospheres of giant planets of our own solar system, or for extra-solar planets.

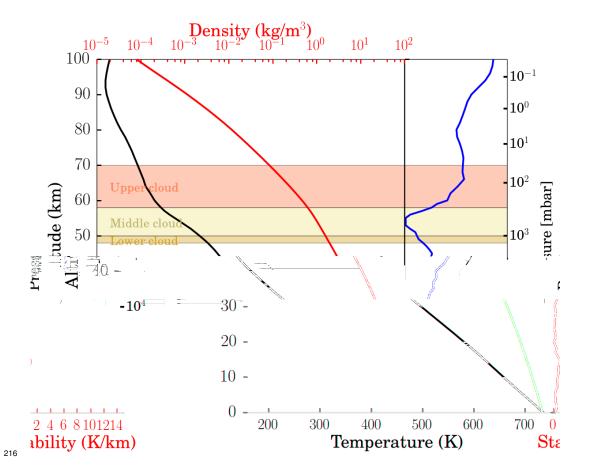
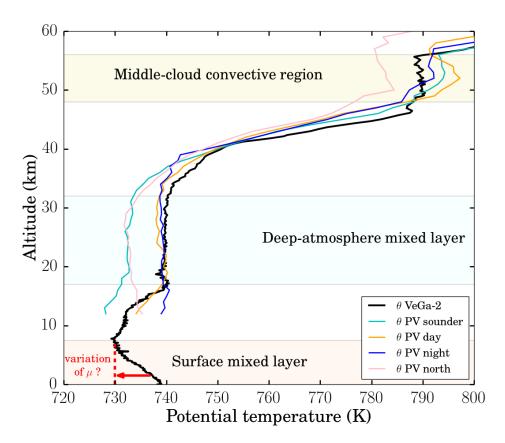


Figure 1 | Vertical structure of the atmosphere of Venus. Vertical profiles, as a function of altitude and pressure, of the temperature, density and static stability (i.e., the difference between the vertical gradient of temperature and the adiabatic lapse rate), from the Venus International Reference Atmosphere model.<sup>22</sup> Cloud layers are also indicated.



Figure 2 | The VeGa-2 spacecraft. Model of the VeGa spacecraft, with the lander visible in the top spherical shell (Lavochkin Museum, near Moscow). Image credits: Lavochkin Association.



224

226

227

228

229

Figure 3 | Vertical profile of potential temperature  $\theta$  computed from temperatures mea-225 sured by VeGa-2. Potential temperature is computed using Eq. S10 in the online Methods. VeGa-2 profile shows the convective layer present in the middle and lower clouds (48-56 km altitude), observed in all in-situ and radio-occultation datasets, 14,22 as well as a deep-atmosphere mixed layer (17-32 km altitude), consistent with the Venus International Reference Atmosphere (VIRA) model<sup>22</sup> and the Pioneer Venus Sounder, Day and Night probes.<sup>16</sup> The highly unstable 7-km thick surface layer is also highlighted ( $\mu$  is the mean molecular mass of the atmosphere).

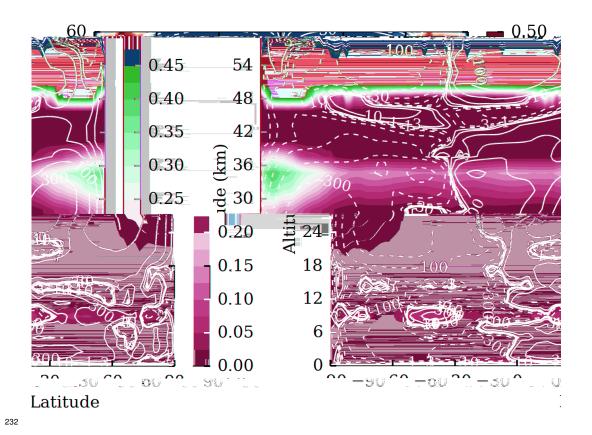


Figure 4  $\mid$  Meridional distributions of the turbulent mixing coefficient and averaged stream

233

function. The diurnal and zonal average of the turbulent mixing coefficient  $K_z$  diagnosed in the GCM is shown with colors (unit is m<sup>2</sup>/s), showing convective regions, while the mean meridional circulation is illustrated by the averaged stream function with the white contours (unit is  $10^9$  kg/s). The amplitude of  $K_z$  reaches more than 10 m<sup>2</sup>/s in the cloud turbulent layer (48-57 km).

#### 39 **Box 1**

249

250

251

259

The stability of an atmospheric region is assessed by moving adiabatically an air parcel along the vertical. For an ideal gas, its temperature follows the adiabatic lapse rate  $\left(\frac{dT}{dz}\right)_{adiab} = \Gamma = -\frac{g}{c_p}$ , 241 where g is the gravity and  $c_p$  is the specific heat capacity at constant pressure. In a well mixed 242 atmosphere (constant molecular mass  $\mu$ ), if the parcel rises to a colder environment (or sinks 243 to a warmer environment), it will continue to rise (or sink), becoming buoyant and triggering convective activity. This corresponds to a vertical temperature gradient lower than the adiabatic 245 lapse rate. The stability can then be assessed with the static stability:  $S = \frac{dT}{dz} - \Gamma$ : when S is 246 positive, the atmosphere is stable, but when S is negative, convective activity will mix energy 247 and modify the temperature profile until S=0. 248

The potential temperature  $\theta$  is defined as the temperature that an air parcel would get after undergoing an adiabatic displacement from its position (T,p) to a reference pressure  $p_{ref}$ . The static stability S is equivalent to the vertical gradient of the potential temperature,  $\frac{1}{\theta} \frac{d\theta}{dz}$ .

When the mean molecular mass is not constant with altitude, to define the buoyancy of a given parcel, the relevant variable is the potential density  $\rho_{\theta}$ , defined as the density a parcel with the density  $\rho(\mu, T, p)$  would have when displaced adiabatically (and with constant composition) to the reference pressure  $p_{ref}$ ,  $\rho_{\theta}(\mu, \theta, p_{ref})$ . In the case of the deep atmosphere of Venus, the stability criterion can be reduced to the usual criterion, but applied to the modified potential temperature  $\theta' = \theta(\mu_{ref}/\mu)$ , with  $\mu_{ref} = 43.44$  g/mol a reference value corresponding to CO<sub>2</sub> mixed with 3.5% of N<sub>2</sub>:  $\frac{1}{\theta'} \frac{d\theta'}{dz} \geq 0$ .

Additional details may be found in the online Methods section.

## • References

- 1. Crisp, D. & Titov, D. The thermal balance of the Venus atmosphere. In S. W. Bougher,
- D. M. Hunten and R. J. Phillips (ed.) Venus II, geology, geophysics, atmosphere, and solar
- wind environnement, 353–384 (Univ. of Arizona Press, 1997).
- 264 2. von Zahn, U., Kumar, S., Niemann, H. & Prinn, R. Composition of the Venus atmosphere.
- In D. M. Hunten, L. Colin, T. M. Donahue and V. I. Moroz (ed.) Venus, 299–430 (Univ. of
- Arizona Press, 1983).
- 3. Taylor, F. W., Crisp, D. & Bézard, B. Near-infrared sounding of the lower atmosphere
- of Venus. In S. W. Bougher, D. M. Hunten and R. J. Phillips (ed.) Venus II, geology,
- geophysics, atmosphere, and solar wind environnement, 325–351 (Univ. of Arizona Press,
- 270 1997).
- 4. de Bergh, C. et al. The composition of the atmosphere of Venus below 100km altitude: An
- overview. *Planet. & Space Sci.* **54**, 1389–1397 (2006).
- 5. Esposito, L. W., Knollenberg, R. G., Marov, M. I., Toon, O. B. & Turco, R. P. The clouds
- and hazes of Venus, 484–564 (Univ. of Arizona Press, 1983).
- 6. Oertel, D. et al. Infrared spectrometry of Venus from Venera-15 and Venera-16. Adv. Space
- 276 Res. 5, 25–36 (1985).
- 7. Moroz, V. I., Linkin, V. M., Matsygorin, I. A., Spaenkuch, D. & Doehler, W. Venus space-
- craft infrared radiance spectra and some aspects of their interpretation. Appl. Opt. 25,
- 279 1710–1719 (1986).

- 8. Yakovlev, O. I., Matyugov, S. S. & Gubenko, V. N. Venera-15 and -16 middle atmosphere profiles from radio occultations: Polar and near-polar atmosphere of Venus. *Icarus* **94**, 493–510 (1991).
- 9. Kliore, A. J. & Patel, I. R. Vertical structure of the atmosphere of Venus from Pioneer Venus orbiter radio occultations. *J. Geophys. Res.* **85**, 7957–7962 (1980).
- <sup>285</sup> 10. Taylor, F. W. *et al.* Structure and meteorology of the middle atmosphere of Venus: Infrared remote sounding from the Pioneer Orbiter. *J. Geophys. Res.* **85**, 7963–8006 (1980).
- <sup>287</sup> 11. Hinson, D. P. & Jenkins, J. M. Magellan radio occultation measurements of atmospheric waves on Venus. *Icarus* **114**, 310–327 (1995).
- Drossart, P. *et al.* Scientific goals for the observation of Venus by VIRTIS on ESA/Venus
   Express mission. *Planet. & Space Sci.* 55, 1653–1672 (2007).
- 291 13. Bertaux, J.-L. *et al.* SPICAV on Venus Express: Three spectrometers to study the global structure and composition of the Venus atmosphere. *Planet. & Space Sci.* **55**, 1673–1700 (2007).
- 14. Tellmann, S., Pätzold, M., Hausler, B., Bird, M. K. & Tyler, G. L. Structure of the Venus
   neutral atmosphere as observed by the radio science experiment VeRa on Venus Express.
   J. Geophys. Res. 114, E00B36 (2009).
- 15. Keldysh, M. V. Venus exploration with the Venera 9 and Venera 10 spacecraft. *Icarus* **30**, 605–625 (1977).
- of Venus and related dynamical observations Results from the four Pioneer Venus probes. *J. Geophys. Res.* **85**, 7903–7933 (1980).

- 17. Linkin, V. M. *et al.* Vertical thermal structure in the Venus atmosphere from provisional Vega 2 temperature and pressure data. *Sov. Astron. Lett.* **12**, 40–42 (1986).
- 18. Linkin, V. M., Blamont, J., Deviatkin, S. I., Ignatova, S. P. & Kerzhanovich, V. V. Thermal structure of the Venus atmosphere according to measurements with the Vega-2 lander.

  Kosm. Issled. 25, 659–672 (1987).
- 19. Bezard, B., de Bergh, C., Crisp, D. & Maillard, J.-P. The deep atmosphere of Venus revealed by high-resolution nightside spectra. *Nature* **345**, 508–511 (1990).
- 20. Pollack, J. B. *et al.* Near-infrared light from Venus' nightside A spectroscopic analysis. *Icarus* **103**, 1–42 (1993).
- 21. Meadows, V. S. & Crisp, D. Ground-based near-infrared observations of the Venus nightside: The thermal structure and water abundance near the surface. *J. Geophys. Res.* **101**,
  4595–4622 (1996).
- 22. Seiff, A., Schofield, J. T., Kliore, A. J. *et al.* Model of the structure of the atmosphere of Venus from surface to 100 km altitude. *Adv. Space Res.* **5**, 3–58 (1985).
- 23. Zasova, L. V., Ignatiev, N. I., Khatuntsev, I. A. & Linkin, V. Structure of the Venus atmosphere. *Planet. & Space Sci.* **55**, 1712–1728 (2007).
- 24. Hoffman, J. H., Oyama, V. I. & von Zahn, U. Measurement of the Venus lower atmosphere composition A comparison of results. *J. Geophys. Res.* **85**, 7871–7881 (1980).
- 25. von Zahn, U. & Moroz, V. Composition of the Venus atmosphere below 100 km altitude.

  Adv. Sp. Res. 5, 173–195 (1985).
- <sup>322</sup> 26. Avduevskii, V. S. *et al.* Automatic stations Venera 9 and Venera 10 Functioning of descent vehicles and measurement of atmospheric parameters. *Cosmic Res.* **14**, 655–666 (1977).

- 27. Zasova, L. V., Moroz, V. I., Linkin, V. M., Khatuntsev, I. V. & Maiorov, B. S. Structure of the Venusian atmosphere from surface up to 100 km. *Cosmic Res.* **44**, 364–383 (2006).
- 28. Seiff, A. & the VEGA Baloon Science Team. Further information on structure of the atmosphere of Venus derived from the VEGA Venus Balloon and Lander mission. *Adv. Space Res.* **7**, 323–328 (1987).
- 29. Gierasch, P. J. *et al.* The general circulation of the Venus atmosphere: an assessment.

  In S. W. Bougher, D. M. Hunten and R. J. Phillips (ed.) *Venus II, geology, geophysics, atmosphere, and solar wind environnement,* 459–500 (Univ. of Arizona Press, 1997).
- 332 30. Hendry, D. *et al.* Exploration of high pressure equilibrium separations of nitrogen and carbon dioxide. *J. CO*<sub>2</sub> *Utilization* **3-4**, 37–43 (2013).
- 31. Spiga, A., Forget, F., Lewis, S. R. & Hinson, D. P. Structure and dynamics of the convective boundary layer on Mars as inferred from large-eddy simulations and remote-sensing measurements. *Q. J. R. Meteorol. Soc.* **136**, 414–428 (2010).
- 337 32. Read, P. L. *et al.* Global energy budgets and 'Trenberth diagrams' for the climates of terrestrial and gas giant planets. *Quater. J. R. Met. Soc.* **142**, 703–720 (2016).
- 33. Wordsworth, R. D. Atmospheric nitrogen evolution on Earth and Venus. *Earth and Planet*.

  340 *Sci. Lett.* **447**, 103–111 (2016).
- 34. Espanani, R., Miller, A., Busick, A., Hendry, D. & Jacoby, W. Separation of N<sub>2</sub>/CO<sub>2</sub>
  mixture using a continuous high-pressure density-driven separator. *J. CO<sub>2</sub> Utilization* **14**,
  67–75 (2016).

- 35. Span, R. & Wagner, W. A New Equation of State for Carbon Dioxide Covering the Fluid
  Region from the Triple-Point Temperature to 1100 K at Pressures up to 800 MPa. *J. Phys.*Chem. Ref. Data 25, 1509–1596 (1996).
- 36. Landau, L. D. & Lifshitz, E. M. *Course of Theoretical Physics vol. 6: Fluid mechanics*(Pergamon Press, Oxford, UK, 1959).
- 37. Lebonnois, S., Sugimoto, N. & Gilli, G. Wave analysis in the atmosphere of Venus below 100-km altitude, simulated by the LMD Venus GCM. *Icarus* **278**, 38–51 (2016).
- 38. Lebonnois, S., Eymet, V., Lee, C. & Vatant d'Ollone, J. Analysis of the radiative budget of Venus atmosphere based on infrared Net Exchange Rate formalism. *J. Geophys. Res.*Planets 120, 1186–1200 (2015).
- 39. Charnay, B. & Lebonnois, S. Two boundary layers in Titan's lower troposphere inferred from a climate model. *Nature Geosci.* **5**, 106–109 (2012).

## 356 Acknowledgements

The authors thank Ludmila Zasova for providing the VeGa-2 probe temperature profile, and Josette Bellan for mentioning barodiffusion and useful discussion on this phenomenon. S.L. acknowledges the support of the Centre National d'Etudes Spatiales. G.S. acknowledges the support of the Keck Institute for Space Studies under the project "Techniques and technologies for investigating the interior structure of Venus".

#### 362 Methods

#### Stability and potential temperature

The stability of an air parcel undergoing an adiabatic displacement in situations where  $\mu$  and/or  $c_p$  may depend on altitude, pressure or temperature is detailed in the following study. The notations used are as follows: R is the universal gas constant (R=8.3144621 J mol $^{-1}$ K $^{-1}$ ),  $\mu$  is the mean molecular mass, p is the pressure,  $\rho$  is the density,  $v=1/\rho$  is the specific volume, T is the temperature,  $c_p$  and  $c_v$  are the specific heat capacities at constant pressure and constant volume,  $\lambda = c_p/c_v$  and  $\kappa = R/(\mu c_p)$ .

370 **Initial equations.** The basic equations for this study are:

- the specific heat relations

372 (Eq. S1)

$$dU = c_v dT$$

373 (Eq. S2)

$$\frac{R}{\mu} = c_p - c_v$$

374 which yields

$$\kappa = 1 - \frac{1}{\lambda}$$

- the first law of thermodynamics for adiabatic displacement

376 (Eq. S3)

$$dU = -pdv$$

- the equation of state for an ideal gas

378 (Eq. S4)

$$\rho = \frac{\mu p}{RT}$$

Note that in the case of the deep atmosphere of Venus, the ideal gas law is only an approximation, but with an error on density less than 0.8% (Table S1).  $^{19,35}$ 

- the hydrostatic balance

382 (Eq. S5)

$$dp = -\rho g dz$$

When  $\mu$  is constant in the atmosphere. In the cases where  $\mu$  is constant in the atmosphere,

Eq. S4 can be written as:

$$pv = \frac{R}{\mu}T$$

Differentiating this equation yields

386 (Eq. S6)

$$pdv + vdp = \frac{R}{\mu}dT$$

From Eqs. S1 and S3, we get

$$pdv = -c_v dT$$

Together with Eq. S2, Eq. S6 becomes

$$vdp = c_n dT$$

Using Eq. S4 again, this yields

390 (Eq. S7)

$$\frac{R}{\mu}\frac{dp}{p} = c_p \frac{dT}{T}$$

The potential temperature  $\theta$  is defined as the temperature that an air parcel would get after undergoing an adiabatic displacement to a reference pressure  $p_{ref}$ . Its expression is obtained by integrating this adiabatic displacement from (T,p) to  $(\theta,p_{ref})$ . When  $c_p$  is constant, Eq. S7 yields the usual expression

$$\theta = T \left( \frac{p_{ref}}{p} \right)^{\kappa}$$

When  $c_p$  depends on the temperature, the integration is not direct. Using the expression

397 (Eq. S9)

$$c_p = c_{p0} \left(\frac{T}{T_0}\right)^{\nu}$$

(with  $c_{p0}$ =1000 J/kg/K,  $T_0=460$  K and  $\nu=0.35$  for Venus' atmosphere),  $^{35,40,41}$  it can be demonstrated that the new expression for  $\theta$  is:

400 (Eq. S10)

$$\theta^{\nu} = T^{\nu} + \nu T_0^{\nu} ln \left(\frac{p_{ref}}{p}\right)^{\kappa_0}$$

with  $\kappa_0 = R/(\mu c_{p0})$ .

Using Eqs. S4, S5 and S7 yields

$$-\frac{gdz}{T} = c_p \frac{dT}{T}$$

which gives the adiabatic lapse rate (valid even for variable  $c_p$ )

404 (Eq. S11)

408

$$\left(\frac{dT}{dz}\right)_{adiab} = \Gamma = -\frac{g}{c_p}$$

When  $\mu$  depends on altitude, pressure or temperature. The stability criterion is established as follows. 42,43 Consider a parcel that is displaced adiabatically on an elemental distance dz, q\* refers to the variable q in the parcel.

Eq. S4 can be written as

$$p*\mu* = \rho*RT*$$

Taking the logarithm then differentiating along the vertical axis ( $\mu$ \* is constant because the composition of the parcel does not change) yields

$$\frac{1}{p*}\frac{dp*}{dz} = \frac{1}{\rho*}\frac{d\rho*}{dz} + \frac{1}{T*}\frac{dT*}{dz}$$

Using Eq. S7 applied to the parcel and p = p\* yields

412 (Eq. S12)

$$\frac{1}{\rho *} \frac{d\rho *}{dz} = \frac{1}{p} \frac{dp}{dz} (1 - \kappa *)$$

with  $\kappa * = R/(\mu * c_p)$ .

414 For the background gas, Eq. S4 can be written as:

$$\rho = \frac{\mu p}{RT}$$

Taking the logarithm then differentiating along the vertical axis yields

416 (Eq. S13)

$$\frac{1}{\rho}\frac{d\rho}{dz} = \frac{1}{\mu}\frac{d\mu}{dz} + \frac{1}{p}\frac{dp}{dz} - \frac{1}{T}\frac{dT}{dz}$$

The stability criterion is

418 (Eq. S14)

$$\frac{1}{\rho *} \frac{d\rho *}{dz} > \frac{1}{\rho} \frac{d\rho}{dz}$$

Eqs. S12 and S13 yield

420 (Eq. S15)

$$\frac{1}{\mu}\frac{d\mu}{dz} - \frac{1}{T}\frac{dT}{dz} + \frac{\kappa *}{p}\frac{dp}{dz} < 0$$

Applying this stability criterion, the adiabatic lapse rate is obtained when neutral for stabil-

422 ity:

423 (Eq. S16)

$$\frac{1}{\mu}\frac{d\mu}{dz} - \frac{1}{T}\frac{dT}{dz} + \frac{\kappa *}{p}\frac{dp}{dz} = 0$$

Using Eqs. S4, S5 and the fact that  $\kappa/\kappa*$  tends to 1 for an elemental displacement, this can

be written as

426 (Eq. S17)

$$\left(\frac{dT}{dz}\right)_{adiab} = \Gamma = \frac{T}{\mu} \frac{d\mu}{dz} - \frac{g}{c_p}$$

which is valid even for variable  $c_p$ .

To define the buoyancy of a given parcel, the relevant variable is the potential density  $\rho_{\theta}$ , defined as the density a parcel with the density  $\rho(\mu,T,p)$  would have when displaced adiabatically (and with constant composition) to the reference pressure  $p_{ref}$ ,  $\rho_{\theta}(\mu,\theta,p_{ref})$ . Using the ideal gas law (Eq. S4), the potential density is

432 (Eq. S18)

$$\rho_{\theta} = \frac{\mu p_{ref}}{R\theta} = \frac{\mu_{ref} p_{ref}}{R\theta'}$$

with the modified potential temperature  $\theta'$  defined by

434 (Eq. S19)

$$\theta' = \theta(\mu_{ref}/\mu)$$

Due to the variation of  $\mu$  with altitude and the dependence of  $\theta$  on  $\mu$ , it is not correct to reduce the stability criterion (Eq. S16) to the usual criterion, i.e., the direct comparison of the potential density between two atmospheric levels.<sup>44</sup>

438 (Eq. S20)

$$\frac{1}{\rho_{\theta}} \frac{d\rho_{\theta}}{dz} = \frac{1}{\mu} \frac{d\mu}{dz} - \left(\frac{1}{\theta} \frac{\partial \theta}{\partial z}\right)_{\mu} - \left(\frac{1}{\theta} \frac{\partial \theta}{\partial \mu}\right)_{z} \frac{d\mu}{dz}$$

For an elemental displacement, the definition of  $\theta$  yields

440 (Eq. S21)

$$\left(\frac{1}{\theta}\frac{\partial\theta}{\partial z}\right)_{\mu} = \frac{1}{T}\frac{dT}{dz} - \frac{\kappa * dp}{p}\frac{dz}{dz}$$

which can be inserted in Eq. S20 to give

442 (Eq. S22)

$$\frac{1}{\rho_{\theta}} \frac{d\rho_{\theta}}{dz} = \frac{1}{\mu} \frac{d\mu}{dz} - \frac{1}{T} \frac{dT}{dz} + \frac{\kappa *}{p} \frac{dp}{dz} - \left(\frac{1}{\theta} \frac{\partial \theta}{\partial \mu}\right)_{z} \frac{d\mu}{dz}$$

Eq. S22 shows that  $d\rho_{\theta}/dz=0$  (or  $d\theta'/dz=0$ ) is not equivalent to the stability criterion (Eq. S16), unless the last term of the right side is negligible against the first.

However, in the case of the deep atmosphere of Venus, the vertical profile of  $\theta(\mu)$  is very close (difference less than 0.15 K everywhere) to the profile of  $\theta(\mu_{ref})$ , with  $\mu_{ref}=43.44$  g/mol a reference value corresponding to  $CO_2$  mixed with 3.5% of  $N_2$ . This yields  $(\mu/\theta)(\partial\theta/\partial\mu)\sim (43.44/735)\times (0.15/0.56)\sim 0.016$ , much smaller than 1. It is therefore a good approximation to consider that the definition of the potential temperature  $\theta$  is not dependent on the initial mean molecular mass of the air parcel, i.e.,  $\partial\theta/\partial\mu=0$  at any given level. In this case, the stability criterion is equivalent to the usual criterion applied to the modified potential temperature  $\theta'$ :

(Eq. S23)

452

$$\frac{1}{\theta'}\frac{d\theta'}{dz} = 0.$$

#### **Radiative transfer details**

In the GCM used for our study, the temperature structure is modeled using a full radiative 454 transfer model. In the infrared range, net exchange rate (NER) formalism is used<sup>38,45</sup> based 455 on up-to-date gas opacities including collision-induced absorption from CO<sub>2</sub> dimers<sup>46</sup>, and the 456 most recent cloud model deduced from Venus-Express datasets<sup>47</sup>. In the solar range, vertical 457 profiles of the solar fluxes computed using this new cloud model are used, depending on lati-458 tude and solar zenith angle<sup>48</sup>. As discussed in a recent work<sup>38</sup> extinction coefficients below the 459 clouds in windows located between 3 and 7 microns play a key role in shaping the deep atmo-460 sphere temperature profile. The solar heating profile below the clouds is also crucial, though it 461 is poorly constrained by available data. 462

Globally averaged 1-dimensional simulations were performed to assess the sensitivity to crucial hypotheses in the radiative transfer calculation. Different solar heating rate models were used<sup>48–50</sup> (Fig. S1a). The composition of the lower haze particles, located between the cloud base (48 km) and 30 km and observed by the probe nephelometers<sup>51</sup>, is not established, so their optical properties are not well constrained. The absorption of the solar flux in this region is

therefore subject to uncertainty. An increased solar absorption (by a factor 3) in this region in the H15 profile<sup>48</sup> (Fig. S1) provides the best fit to the VIRA and Vega-2 temperature profiles. 469 In the infrared, some additional extinction is needed below the clouds in the 3 to 7 microns wavelength range to fit the temperature profile in the stable region below the clouds<sup>38</sup>. The 471 lower haze, which is not taken into account in the reference NER computations, can contribute 472 to this small additional continuum. The impact of several hypotheses on this additional opacity 473 is illustrated in Fig. S1b. The best fit to the VIRA and Vega-2 temperature profiles is obtained 474 with an additional extinction of  $1.3 \times 10^{-6}$  cm<sup>-1</sup> amagat<sup>-2</sup> in the lower haze region (30-48 km), 475 and of  $4 \times 10^{-7}$  cm<sup>-1</sup> amagat<sup>-2</sup> in the region between 30 and 16 km, where a transition from 476 instability to stability against convection is observed in the Vega-2 profile, but also in the Pioneer 477 Venus Sounder, Day and Night probes at similar altitudes (15 to 20 km)<sup>19</sup>.

#### 479 References

- 40. Lebonnois, S. *et al.* Superrotation of Venus' atmosphere analysed with a full General Circulation Model. *J. Geophys. Res.* **115**, E06006 (2010).
- 41. Poling, B., Prausnitz, J. & O'Connell, J. *The properties of gases and liquids* (McGraw-Hill, 2001).
- 42. Ledoux, P. Stellar models with convection and with discontinuity of the mean molecular weight. *Astrophys. J.* **105**, 305–321 (1947).
- 43. Hess, S. L. Static stability and thermal wind in an atmosphere of variable composition:

  Applications to Mars. *J. Geophys. Res.* **84**, 2969–2973 (1979).
- 44. Pierrehumbert, R. T. *Principles of Planetary Climate* (Cambridge Univ. Press, Cambridge,
   UK, 2010).

- 490 45. Eymet, V. *et al.* Net-exchange parameterization of the thermal infrared radiative transfer in Venus' atmosphere. *J. Geophys. Res.* **114**, E11008 (2009).
- 492 46. Stefani, S., Piccioni, G., Snels, M., Grassi, D. & Adriani, A. Experimental CO<sub>2</sub> absorption 493 coefficients at high pressure and high temperature. *J. of Quantit. Spec. and Rad. Transfer* 494 **117**, 21–28 (2013).
- 47. Haus, R., Kappel, D. & Arnold, G. Atmospheric thermal structure and cloud features in the southern hemisphere of Venus as retrieved from VIRTIS/VEX radiation measurements. *Icarus* **232**, 232–248 (2014).
- 48. Haus, R., Kappel, D. & Arnold, G. Radiative heating and cooling in the middle and lower atmosphere of Venus and responses to atmospheric and spectroscopic parameter variations. *Planet. & Space Sci.* **117**, 262–294 (2015).
- 49. Crisp, D. Radiative forcing of the Venus mesosphere. I Solar fluxes and heating rates. *Icarus* 67, 484–514 (1986).
- 50. Lee, C. & Richardson, M. I. A Discrete Ordinate, Multiple Scattering, Radiative Transfer

  Model of the Venus Atmosphere from 0.1 to 260μm. *J. Atm. Sci.* **68**, 1323–1339 (2011).
- 51. Knollenberg, R. G. *et al.* The clouds of Venus: A synthesis report. *J. Geophys. Res.* 85,
   8059–8081 (1980).

#### Data and code availability

- The VeGa-2 temperature profile was provided kindly provided by Ludmila Zasova. It is available from the corresponding author upon request.
- The LMD Venus GCM used in this study is developed in the corresponding author's team.

  It is also available upon request.

## **Author contributions**

Both authors contributed equally to the manuscript.

## 514 Additional information

- Methods section and Supplementary Information are available in the online version of the paper.
- Correspondence and requests for materials should be addressed to S.L.

# **Competing financial interests**

The authors declare no competing financial interests.